# Assessment of heat transport and distribution in the high Arctic in eddy resolving model

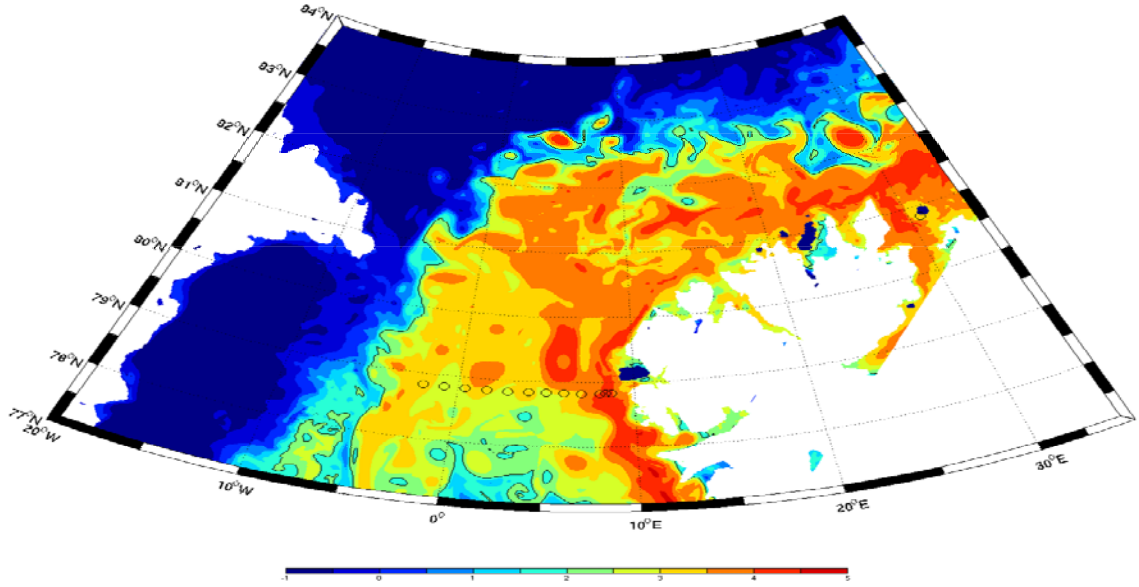


Temperature at 100 meters in a high resolution ice-ocean model . Credits: Christophe Herbaut, CNRS

**We support Blue Growth!**

**Visit us on:** www.blue-action.eu
**Follow us on Twitter**: @BG10Blueaction

**Blue-Action: Arctic Impact on Weather and Climate** is a Research and Innovation action (RIA) funded by the Horizon 2020 Work programme topics addressed: BG-10-2016 Impact of Arctic changes on the weather and climate of the Northern Hemisphere. Start date: 1 December 2016. End date: 1 March 2021.

The Blue-Action project has received funding from the European Union's Horizon 2020 Research and Innovation Programme under Grant Agreement No 727852.

**Milestone:** MS8
**Work package in charge:** WP2: Lower latitude drivers of Arctic changes
**Actual achievement date of this milestone:** Project-month 29

**Partner organisation in charge of the milestone and lead authors**
Centre National de la Recherche Scientifique (CNRS): Christophe Herbaut, Marie-Noelle Houssais, Anne-Cécile Blaizot

**Reviewers**
Faroe Marine Research Institute (HAV): Karin Margretha H. Larsen
National University of Ireland Maynooth (NUIM): Gerard McCarthy

**Milestone Type:** Report

**Dissemination level:** Public

**Means of verification of attainment of the milestone**
Identification of robust metrics**:**

- the mean Atlantic Water temperature,
- the Atlantic Water section area,
- the Atlantic Water heat content and
- the heat and volume transports.

**Achieved:** Yes

## Contents

## Introduction

The decline of Arctic sea ice in the recent decades is regionally dependent, with an increasing trend since the mid 2000s in the Eurasian Basin (Close et al., 2015). The increase of the oceanic heat flux has been suggested to be the main driver of this ice loss in the eastern Eurasian Basin, with an estimated contribution of 40-50 cm in ice growth reduction in the recent years (Polyakov et al., 2017). According to these authors, the decrease of the stability in the halocline and the shoaling of the **Atlantic Water (AW)** interface, often referred to as the Atlantification of the Eurasian Basin, altogether have provided favorable conditions for increased ocean heat transfer towards the surface. The source of these changes should be found in the region north of Svalbard where the warm AW inflowing through the Fram Strait first encounters the sea ice, being responsible for increased sea ice melt in the recent period.

Our goal in the Blue Action project is to investigate how the heat provided by the Atlantic inflow through Fram Strait is subsequently modified along its pathway in the southern Eurasian Basin and to which extent its distribution controls the amount of heat which is transferred to the surface layer and ultimately to the sea ice. The analysis which is presented in this milestone focuses on the region around Svalbard to evaluate the upstream conditions at the entrance of the Arctic Ocean. It relies on results of a model simulation carried out using a 1/24° ocean-sea ice model. The results have been compared to in-situ observations (collected from moorings and shipborne CTD (Conductivity-Temperature-Depth)) in order to identify the metrics which are the more relevant to characterize the Atlantic water layer. The considered metrics are related to the heat content and transports of AW. They are used to assess the model ability to represent the observations.

The AW is originally carried towards the Arctic Ocean by the West Spitzbergen Current (WSC) (Walczowski et al., 2016) and a first comparison between model and observations has been made in Fram Strait where long term observations are available (Beszczynska-Möller, et al., 2012). In Fram Strait, part of the northward flow of AW recirculates southward while, north of the strait, the flow separates into two branches: the Svalbard branch continues along the upper Svalbard slope, veering eastwards to enter the Eurasian Basin; the Yermak branch, on the other hand, flows northwestwards and continues around the Yermak Plateau. The actual amount of heat which ultimately enters the Arctic Ocean is therefore dependent on the flow partition between these different branches. To investigate the link between the AW flow in the WSC and the AW flow in the Arctic Ocean, we additionally examine the AW distribution at two locations in the Eurasian basin where sparser mooring and CTD data have been collected (Dmitrenko et al., 2011, Ivanov et al. 2009) and we try to relate the variability at these locations to that observed in Fram Strait (see Fig.1 for the locations of the sections).

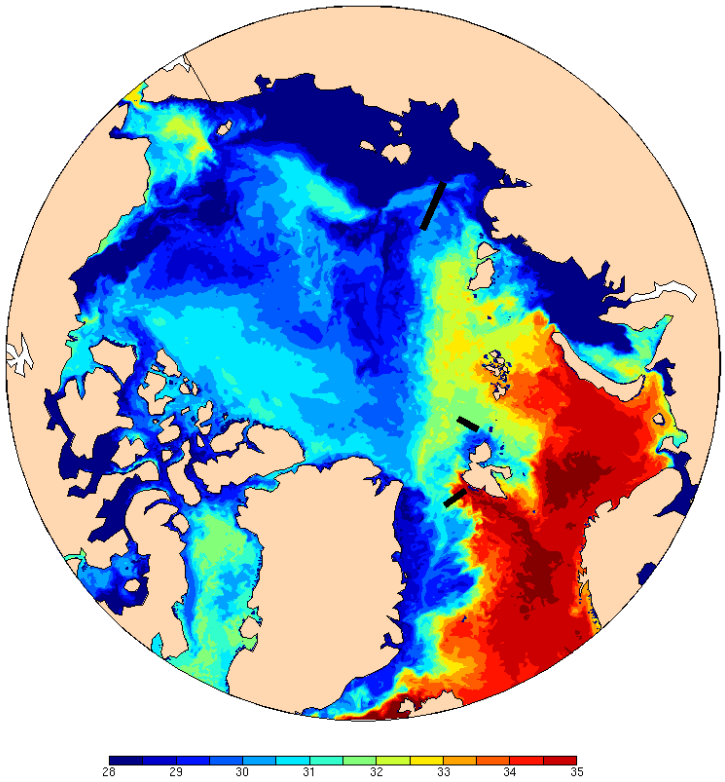


**Figure 1: The locations of the sections (black lines) are superposed on the surface salinity at the end of September 2008 simulated by the model.**

**The high resolution simulation**

A 1/24° ice-ocean model configuration of the Arctic Ocean and the Atlantic Subpolar Gyre has been developed based on NEMO 3.6. The model domain extends from 28°N in the Atlantic Ocean to the Bering Strait**.** At the lateral boundaries, the model is forced by 5-day averaged oceanic conditions from a ¼° global simulation. In the vertical, the equations are discretized on 75 levels with thickness ranging for 1 m at the surface to 250 m at depth. The horizontal resolution in Fram Strait and north of Svalbard is around 2.5 km. The atmospheric forcing fields are based on the ERA-interim reanalysis (Dee et al., 2011), with some corrections applied to precipitation (DFS5, Dussin et al., 2016) and the surface atmospheric temperature. The ocean temperature and salinity are initialized from PHC3 (Steele et al., 2001). We analyze here a simulation over the period 1995-2015 in which the surface salinity restoring which has been imposed over the period 1995-2003 and then removed for the last period of the integration. We focus our analysis on this last period without surface restoring (2004-2015).

**Assessment of Atlantic Water heat content and transport in Fram Strait**

The mooring data from the eastern part of the Fram Strait (east of 3°W) have been uploaded for the period 2004-2011 (doi.org/10.1594/PANGAEA.150016). The extracted dataset is made up of ten moorings which have been deployed along the 78°50'N latitude. The data have been reduced to 5 day averages (to compare with the model data), and an objective analysis has been used to generate sections of temperature and meridional velocity. To compute the heat content, the temperature at the uppermost level of the objective analysis grid has been extended to the surface. The high resolution (up to 5 km on the continental slope) CTD casts collected during six summer cruises of PRV Polarstern

(doi.pangaea.de/10.1594/PANGAEA.845938) were also extracted from the PANGAEA database. A first comparison between the summer conditions in the model and in the CTD observations shows that the model reproduces the overall distribution of the hydrographic properties in Fram Strait, in particular the front which defines the outer limit of the WSC in the eastern part of the strait (Fig. 2). However the model seems to underestimate the temperature of the AW layer, defined as water which is warmer than 2°C and saltier than 34.95.

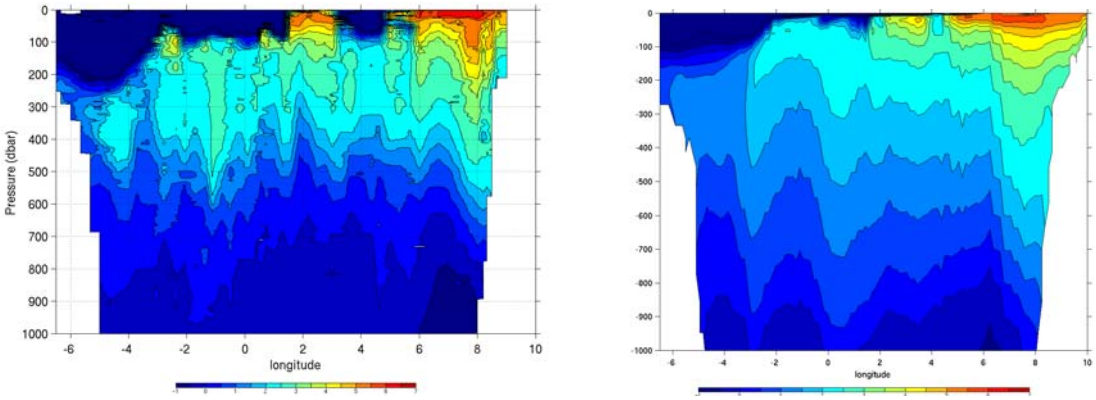


**Figure 2 : Temperature along the 78°50'N in July 2008 (left) from CTD measuremens, (right) in the model.**

An indication of the possible influence of the AW on the surface layer is provided by examining the vertical distribution of the heat content of the upper ocean layers. It is further interesting to determine if this distribution is primarily controlled by the zonal extent of the AW layer or by its mean temperature. Figure 3 shows two contrasted years (2004 being rather warm, while 2008 is cold) regarding this distribution. In the observations, in both years, the mean temperature and the lateral extent in the upper 150 m have opposite vertical gradients, which both contribute to shaping the subsurface maximum of the heat content. Below 300 m the vertical distribution of the heat content is dominated by that of the lateral extent of the AW. The same is found in the model in 2004, where model and observations are in reasonable agreement despite a substantially colder (by about 0.5°C) thermocline in the model. In 2008, however, the model fails to reproduce the depth of the heat content maximum while the match between modelled and observed temperatures is better.

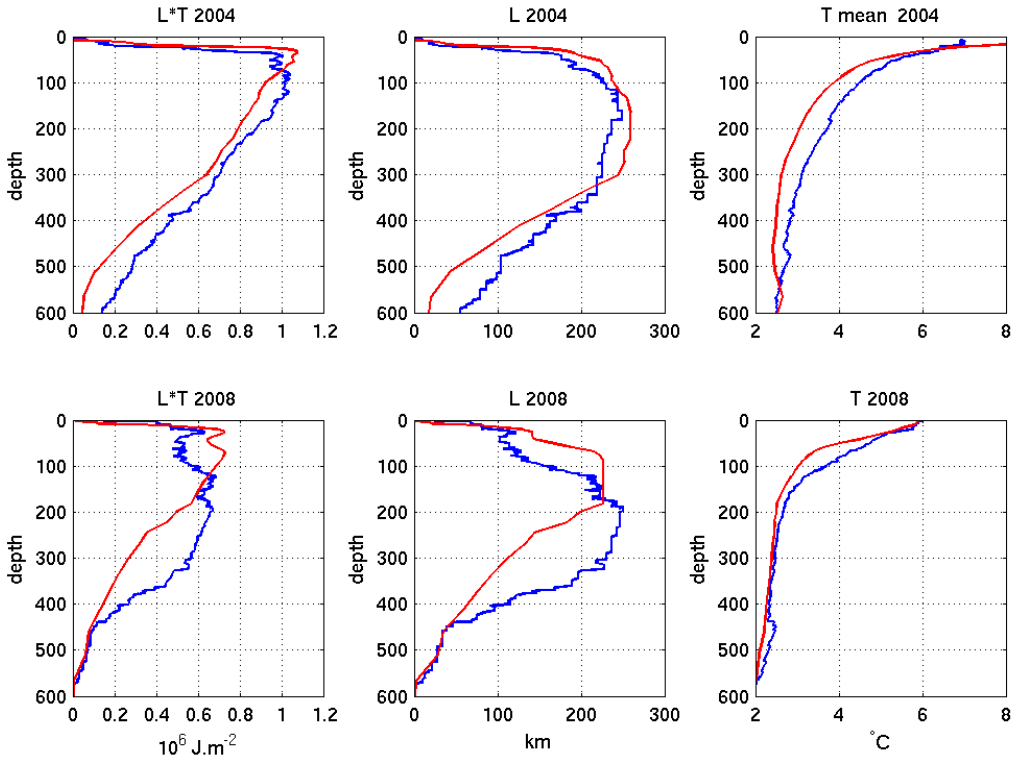


**Figure 3: Vertical distribution of the (left column) heat content, (middle column) zonal extent and (right column) mean temperature of the AW layer for (upper row) summer 2004 and (lower row) summer 2008, from the (red) CTD observations and (blue) model. The profiles are based on integration over the full zonal section across the strait and are typical of summer (July or August) conditions.**

The above profiles only represent summer snapshots and the robustness of the above metrics needs to be ascertained against a full annual cycle. To assess the seasonal cycle of the AW heat content we used the hydrographic observations from the mooring array at 78°50'N. The AW heat content has been computed over the full extent of the array, but also limited to the WSC which constitutes the main flow of AW into the Arctic. The western limit of the WSC was chosen to be 5.5°E based on the temperature decorrelation scale between the onshore mooring at 8.3°E (taken as representative of the WSC variability) and the other moorings located farther offshore. The decorrelation occurs between 5 and 6°E (Fig. 4), in agreement with the definition of the WSC chosen by Beszczynska-Möller et al. (2012).

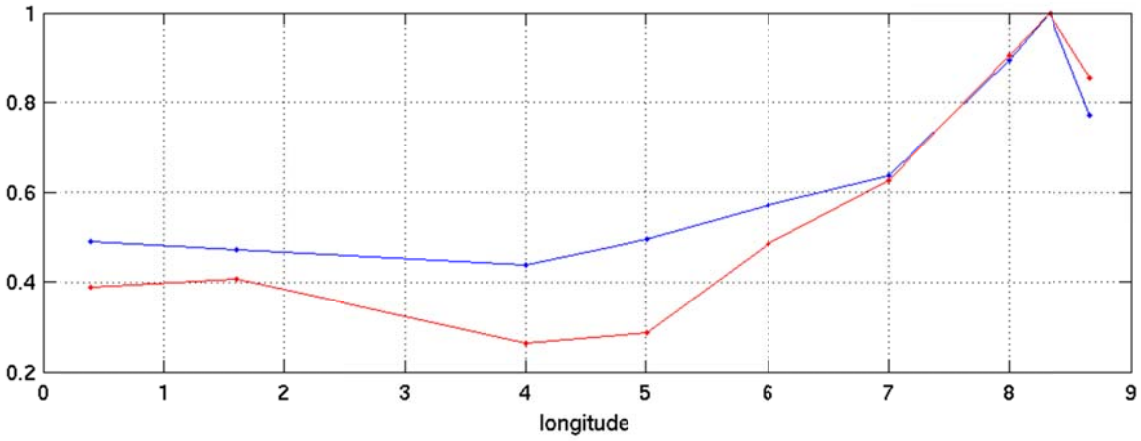


**Figure 4: Correlation of the temperature at 250 meters at the mooring located at 8.3°W with the 250 m temperature measured at the others moorings for the periods 2004-2010 (blue) and 2008-2010 (red).**

When comparing the model and the observations over the full section, the mean AW temperature appears too cold throughout the year and the amplitude of its annual cycle is reduced due to more underestimated temperatures in summer (Fig. 5). The AW section area also shows a negative bias, contributing with the temperature to an underestimation of the AW heat content. The bias is present in all years but larger from 2009 onward (Fig. 5). Separating the difference in heat content between the contribution of the temperature difference and the area difference between the model and the observations, the two contributions reveal to be equivalent. Looking at the WSC part of the section, the same differences are present as evidenced by the mean annual cycle shown in Figure 6. In contrast, the amplitude of the annual cycle of the AW section area is similar between the model and the observations, yet with a bias of 10-15 $km^2$ between the two datasets (Fig. 5 right). Consequently, the seasonal amplitude of the AW heat content is underestimated in the model mainly as a consequence of the reduced seasonal contrast in the temperature. This discrepancy is larger in some specific years (2007, 2010) (Fig. 5). The variations in the thickness of the AW layer do not show any dominant time scale especially at the annual time scale, most probably because the surface driven seasonal changes do not reach deep enough to alter the lower boundary of the AW layer (Fig. 5, bottom panel).

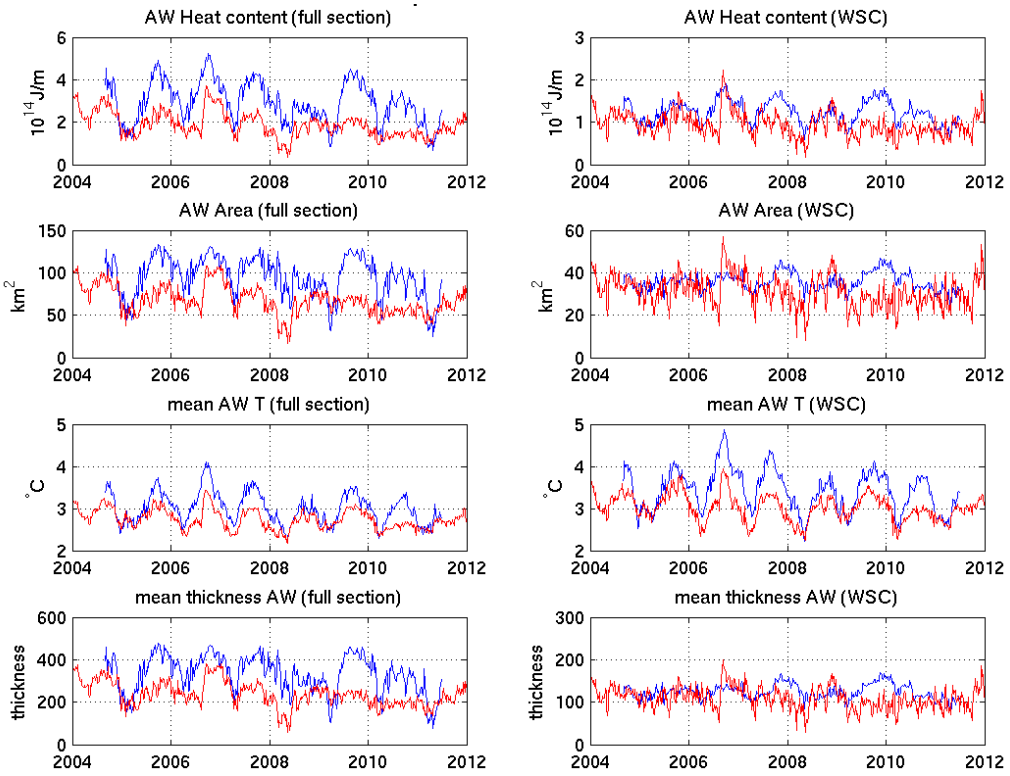


**Figure 5: AW (upper row) heat content, (upper middle row) area, (lower middle row) mean temperature, (lower row) mean thickness for (left column) the full Fram section and (right column) the WSC, for (blue) the observations and (red) the model.**

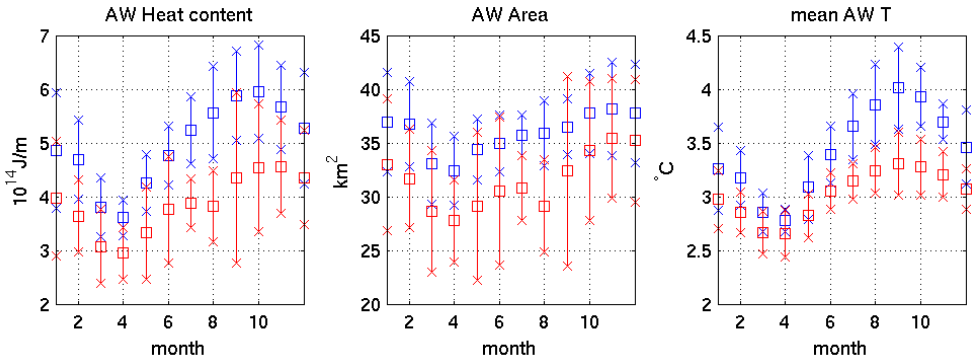


**Figure 6: Long term mean of the monthly AW (left) heat content, (middle) area, and (right) mean temperature in the WSC, for (blue square) the observations and (red square) the model, and their standard deviation.**

Temperatures and velocity measurements at the same moorings have been used to calculate the volume and heat transports associated with the AW in the WSC (remember that these quantities have been first gridded using OA), and to assess the transports simulated by the model (Fig 7). The model simulates the right AW volume inflow. A power spectrum analysis of the velocities at the levels where current measurements are available shows that the model is able to represent the right amount of energy in the full frequency range, except at the mooring which was deployed on the upper part of the Svalbard slope. The agreement is not as good when comparing the transports. The observed transports exhibit much higher (3 times greater) variance than the simulated one, especially at the sub annual cycle

(Fig. 7), most probably as a result of the depth integration which, in the model, is performed over a larger number of levels.

In the observations and in the model, the AW heat transport is well correlated with the volume transport suggesting that the velocity variations are the main driver of the heat transport variability. A wavelet analysis shows that the observed transports are characterized by a strong annual cycle (Fig 8), with a maximum in March and a minimum in July which are correctly reproduced by the model (Fig. 9) and are in agreement with earlier results from Beszczinka-Möller et al (2012).

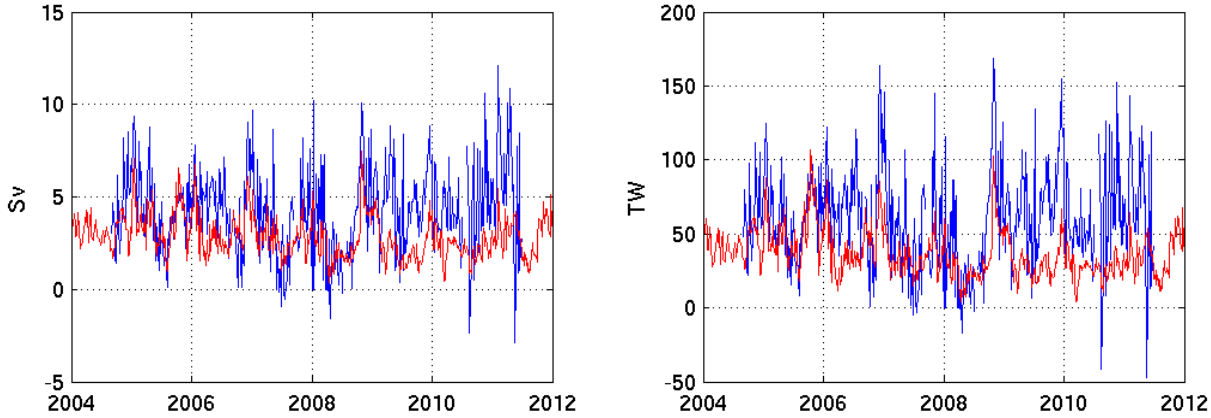


**Figure 7: (left) AW volume and (right) heat transport through Fram Strait from (blue) the observations and (red) the simulation.**

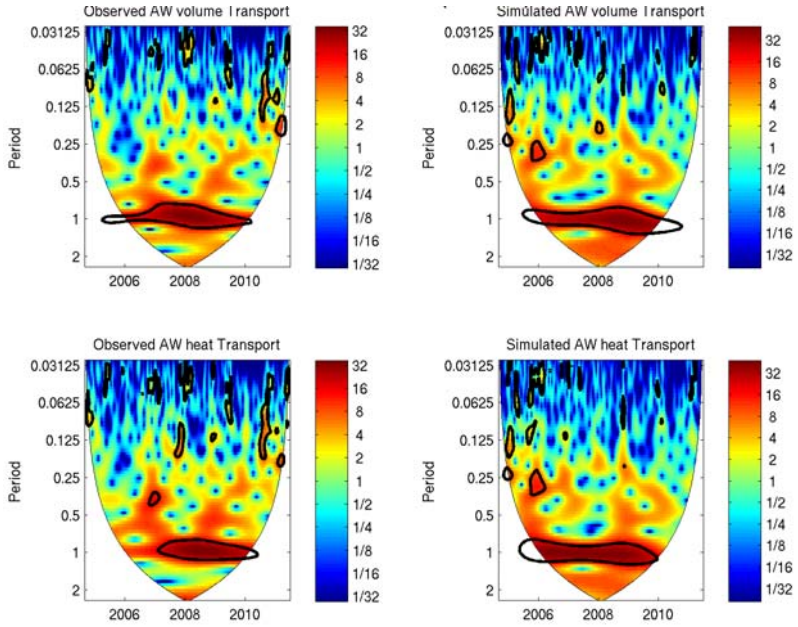


**Figure 8: Wavelet power of (upper row) the AW volume transport and (lower row) AW heat transport in the WSC, (left) in the observations and (right) in the model.**

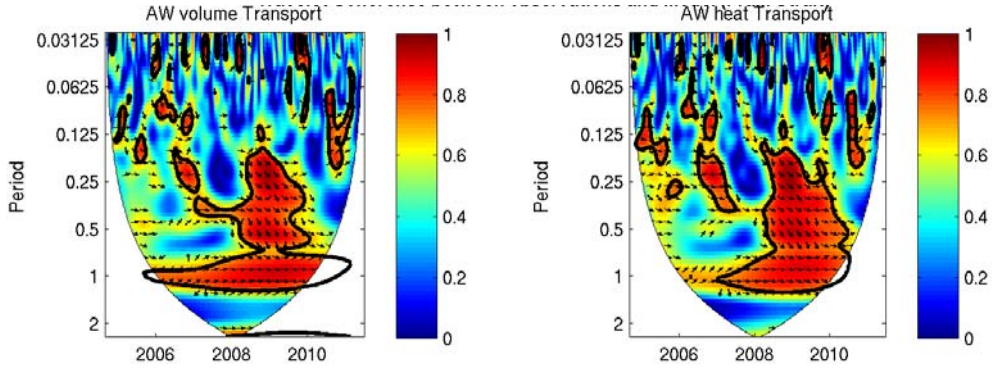


**Figure 9: Wavelet coherence between the observed and simulated (left) AW volume transport and (right) AW heat transport in the WSC.**

**Assessment of Atlantic Water heat content and transport in the Eurasian Basin**

In the Eurasian basin, the observations are sparser than in Fram Strait, and there are no long term measurements. The simulation is thus assessed more qualitatively based on summer hydrographic measurements and mooring data from the NABOS project (http://nabos.iarc.uaf.edu/). At 30°E, the core of the AW is characterized by an intermediate maximum of temperature and salinity which is found between 100 and 500 m and is located on the upper part of the continental slope (Ivanov et al. 2009, Vage et al., 2016) (Fig. 10, upper left panel). Further eastwards in the Eurasian Basin, the structure of the flow is more complex and, since the 2000s, a two core system is observed (Fig. 10, lower left panel), in agreement with earlier studies (Pnyushkov et al., 2015). In the simulation, the core of AW is also identified from the northern slope of Svalbard to the continental slope of the Laptev Seas (Fig 10, right panels) and the main features of the AW are reproduced. The temperature in the AW layer is however too cold at both locations.

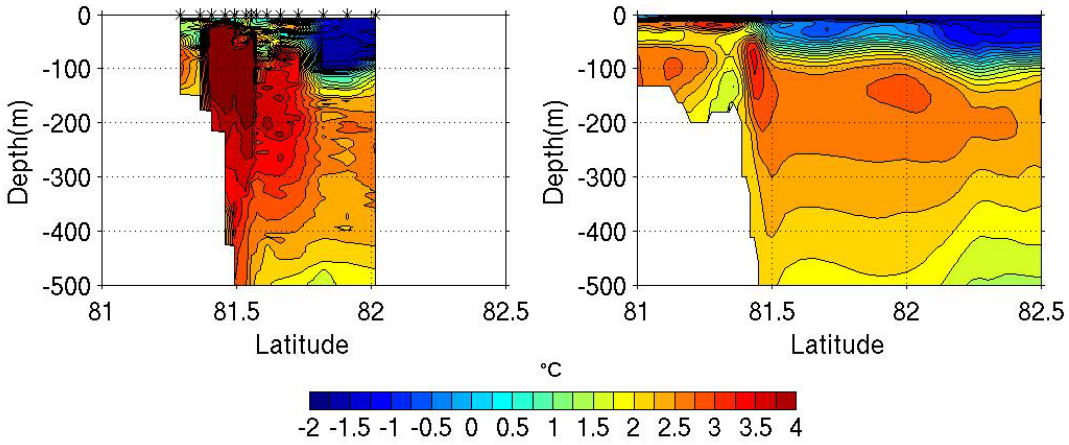

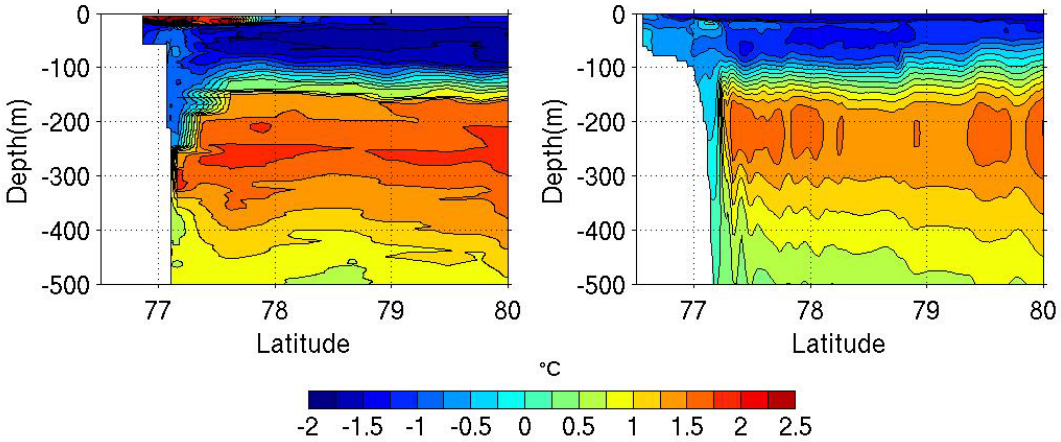


**Figure 10: Vertical section of temperature (upper row) at 30°E in summer 2006 and (lower row) across the Laptev continental slope in summer 2009 in (left column) the observations and (right column) the simulation.**

The AW temperature at 30°E shows a clear annual cycle of about 1°C (Fig. 11). The temperature is usually maximum (with values reaching beyond 3°C) in late autumn and decreases over the winter to reach a minimum in late winter. The temperature remains low in spring (Ivanov et al., 2009, Renner et al, 2018). The temperature minimum in the model is more or less in phase with the observations but a low frequency variability develops which conceals the annual cycle. In agreement with earlier studies, the current at 30°E is more baroclinic than in Fram Strait (Pnyushkov, 2015) and has an horizontal extent of 40-50 km (Pérez-Hernandez et al. 2017) (not shown). The annual cycle of the current velocity in the core of the AW is reasonably reproduced in the model, with a correlation of 0.68 between the simulated and the observed velocities (Fig. 11).

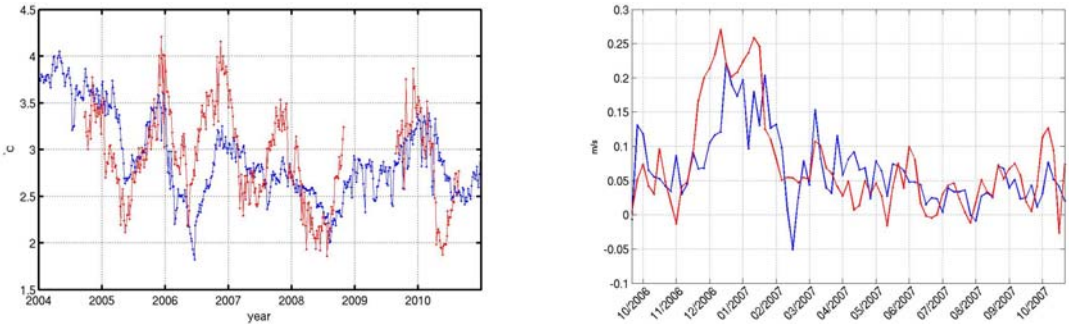


**Figure 11: (left) Temperature at 220 m from (blue) the NABOS mooring located at 30°N on the continental slope and (red) the model. (right) Along slope velocity at 220 m over a one-year period in 2006-2007 from (blue) the NABOS mooring and (red) the model.**

**Link between the Atlantic Water variability in Fram Strait and in the Eurasian Basin**

To analyze how the conditions in Fram Strait influence the conditions downstream of the strait, linear correlations between the current velocities measured at these two locations have been calculated and compared to the same correlations in the model. For the velocity in the core of the Atlantic layer at 30°E, we used two one-year records at 220 m in 2004-2005 and 2006-2007. The velocities have been correlated with the velocities at Fram strait which have been computed with an optimal interpolation. Correlations for the period 2004-2005 are shown in Figure 12. The maximum correlations indicate that the inshore branch of the WSC is the primary source of the AW flow over the Eurasian slope, as was

already mentioned by many authors. However, the short time lag (5 to 15 days) suggests that the variability of the current at the two sites is driven by the same atmospheric pattern or that the Fram Strait variability is transmitted downstream by fast topographic waves. The longer velocity records of the model have been used to calculate correlations between the AW transports at 30°E and in the WSC over the period 2004-2015 (Fig. 12). High correlation (0.78) are found between the transports, both in the low and high frequency range, which suggests that the model is also able to reproduce variability along the path of the AW.

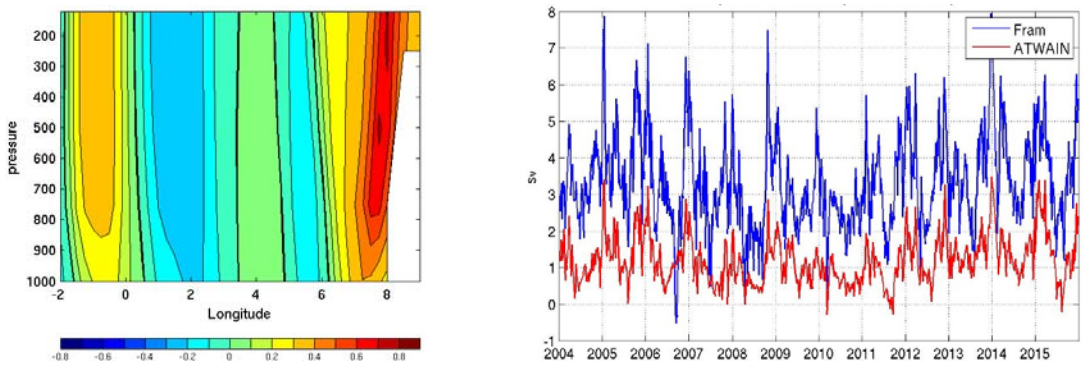


**Figure 12: (Left) Correlation between the velocity at 200 m at the NABOS mooring at 30°E in the Eurasian Basin and the current velocity measured across the mooring network in Fram Strait. Velocities in Fram Strait lead the velocity at 30°E by 5 days. The correlations have been computed over a one-year period in 2004-2005. (Right) AW volume transport (blue) in Fram Strait and (red) at 30°N in the Eurasian Basin in the model. The correlation between the transports is 0.78 at lag 0.**

## Conclusions

To assess the model ability to represent the observed distribution of the AW heat in Fram Strait, we identified the following metrics: the mean AW temperature, the AW section area, and the AW heat content. The model clearly underestimates the AW heat content when the entire width of the strait is considered. However, it agrees better with the observations in the WSC part of the section. The mean temperature and the section area both show a negative bias in the model with the two metrics contributing equally to the model deficiency in terms of heat content.

Due to the shortness of the model simulation, we could not properly assess the interannual variability of the AW. However, the low temperatures which are simulated by the model in 2011 are not found in the observations, suggesting that the model cannot fully capture the actual variability. In contrast, the model shows higher ability to simulate the AW volume and heat transports (the latter being mainly driven by the velocity variations). In the Eurasian Basin, the scarcity of the observations only allows for a qualitative analysis. A short time record of the velocity at a single level in the AW layer at a mooring north of Svalbard indicates that the model is able to reproduce the observations. Additional analyses have to be undertaken in order to characterize the evolution of the AW properties (in particular temperature and heat content) along the AW pathway downstream of Fram Strait, and to determine whether the conditions in Fram Strait are critical for the influence of the AW on the sea ice in the Arctic Basin.

## References

Beszczynska-Möller, A., E. Fahrbach, U. Schauer, and E. Hansen, 2012: Variability in Atlantic water temperature and transport at the entrance to the Arctic Ocean, 1997–2010. ICES Journal of Marine Science: Journal du Conseil, **69 (5)**, 852–863, doi:10.1093/icesjms/fss056.

Close, S., Houssais, M.-N., and Herbaut, C. (2015), Regional dependence in the timing of onset of rapid decline in Arctic sea ice concentration, *J. Geophys. Res. Oceans*, 120, 8077– 8098, doi:10.1002/2015JC011187.

Dee, D. P., Uppala, S. M., Simmons, A. J., Berrisford, P., Poli, P., Kobayashi, S., Andrae, U., Balmaseda, M. A., Balsamo, G., Bauer, P., Bechtold, P., Beljaars, A. C. M., van de Berg, L., Bidlot, J., Bormann, N., Delsol, C., Dragani, R., Fuentes, M., Geer, A. J., Haimberger, L., Healy, S. B., Hersbach, H., Hólm, E. V., Isaksen, L., Kållberg, P., Köhler, M., Matricardi, M., McNally, A. P., Monge-Sanz, B. M., Morcrette, J. J., Park, B. K., Peubey, C., de Rosnay, P., Tavolato, C., Thépaut, J. N., & Vitart, F. (2011). The ERA-interim reanalysis: Configuration and performance of the data assimilation system. Quarterly Journal of the Royal Meteorological Society, 137(656), 553–597. https://doi.org/10.1002/qj.828

Dmitrenko, I. A., Ivanov, V. V., Kirillov, S. A., Vinogradova, E. L., Torres-Valdes, S., & Bauch, D. ( 2011). Properties of the Atlantic derived halocline waters over the Laptev Sea continental margin: Evidence from 2002 to 2009. *Journal of Geophysical Research*, 116, C10024. https://doi.org/10.1029/2011JC007269

Dussin, R., B. Barnier and L. Brodeau, 2016. The making of Drakkar forcing set DFS5. DRAKKAR/MyOcean Report 01-04-16, LGGE, Grenoble, France

Ivanov, V. V., Polyakov, I. V., Dmitrenko, I. A., Hansen, E., Repina, I. A., Kirillov, S. A., et al. (2009). Seasonal variability in Atlantic Water off Spitsbergen. *Deep Sea Research I*, 56, 1– 14. https://doi.org/10.1016/j.dsr.2008.07.013

Pérez-Hernández, M. D., Pickart, R. S., Pavlov, V., Våge, K., Ingvaldsen, R., Sundfjord, A., et al. ( 2017). The Atlantic Water boundary current north of Svalbard in late summer. *Journal of Geophysical Research: Oceans*, 122, 2269– 2290. https://doi.org/10.1002/2016JC012486

Pnyushkov, A. V., Polyakov, I. V., Ivanov, V. V., Aksenov, Y., Coward, A. C., Janout, M., & Rabe, B. ( 2015). Structure and variability of the boundary current in the Eurasian Basin of the Arctic Ocean. *Deep Sea Research I*, 101, 80– 97.

Polyakov, I. V., Pnyushkov, A. V., Alkire, M. B., Ashik, I. M., Baumann, T. M., Carmack, E. C., et al. (2017). Greater role for Atlantic inflows on sea-ice loss in the Eurasian Basin of the Arctic Ocean. *Science*, 356, 285– 291. https://doi.org/10.1126/science.aai8204

Renner, A. H. H., Sundfjord, A., Janout, M. A., Ingvaldsen, R., Beszczynska-Möller, A., Pickart, R., & Pérez-Hernández, M., (2018). Variability and redistribution of heat in the Atlantic Water boundary current north of Svalbard. *Journal of Geophysical Research: Oceans*, 123, 6373– 6391. https://doi.org/10.1029/2018JC013814

Steele M., Morley R., Ermold W.PHC: a global ocean hydrography with a high-quality Arctic Ocean. J. Climate, 14 (2001), pp. 2079-2087

Våge, K., Pickart, R. S., Pavlov, V., Lin, P., Torres, D. J., Ingvaldsen, R., et al. ( 2016). The Atlantic Water boundary current in the Nansen Basin: Transport and mechanisms of lateral exchange. *Journal of Geophysical Research: Oceans*, 121, 6946– 6960. https://doi.org/10.1002/2016JC011715

Walczowski W., A. Beszczynska-Möller, P. Wieczorek, M. Merchel, A. Gryncze 2017). Oceanographic observations in the Nordic Sea and Fram Strait in 2016 under the IO PAN long-term monitoring program AREX, Oceanologia, 59, 187-19. https://doi.org/10.1016/j.oceano.2016.12.003.